

Communication

Effect of Nitrogen Partitioning on Yield Strength in Nitrogen-Alloyed Duplex Stainless Steel During Annealing

MIN-HO JANG, JOONOH MOON, TAE-HO LEE, SEONG-JUN PARK, and HEUNG NAM HAN

Nitrogen partitioning and its effect on the yield strength in nitrogen-alloyed duplex stainless steel during annealing were investigated at different annealing temperatures. The decrease in the austenite fraction with an increase in the annealing temperature promoted nitrogen partitioning into austenite. When the nitrogen content in austenite was low, the yield strength decreased with an increase in the annealing temperature due to grain growth, while when it was higher than 0.5 wt pct, the yield strength increased with an increase in the annealing temperature, because the austenite became noticeably hard.

DOI: 10.1007/s11661-014-2210-8

© The Minerals, Metals & Materials Society and ASM International 2014

Austenitic stainless steel (ASS) has excellent corrosion resistance and high toughness, but it has low yield strength. Ferritic stainless steel (FSS) has high yield strength, though it shows low ductility.^[1] Duplex stainless steels (DSS) are defined as a family of steels consisting of two phase microstructures of ferrite and austenite. Through the optimum mixture of the desirable properties of ASS and FSS, DSS has an attractive combination of good mechanical properties and excellent resistance to stress corrosion cracking.^[1,2]

Extensive studies have done to elucidate the relationship between the phase fraction and the mechanical properties of DSS^[1,3–5]. Park and Lee^[1] and Floreen and Hyden^[3] showed that an increase in the ferrite fraction in DSS resulted in a decrease of the tensile strength and elongation but a linear increase in the yield strength. In addition, Park and Lee^[1] presented empirical models to predict the tensile strength, yield strength, and elonga-

tion as a function of the ferrite fraction. Badji *et al.*^[4] investigated the effect of the annealing temperature on the microstructure and mechanical properties in the weld heat-affected zone (HAZ) of DSS, showing that the yield strength of the weld HAZ increased with an increase in the ferrite fraction.^[4] Unnikrishnan and Mallik^[5] reported that the mechanical properties of DSS depend on the formation of the σ phase at a low annealing temperature [<1273 K (1000 °C)] and the ferrite fraction at a high annealing temperature [>1273 K (1000 °C)]; *i.e.*, the yield strength increases with the formation of the σ phase and an increase of the ferrite fraction.

Many previous studies were interested mainly in the effect of the ferrite fraction on the strengthening of the DSS during a heat treatment, as ferrite is harder, therefore, significantly affecting the strength as compared to austenite. However, a few studies have recently focused on the role of austenite.^[6,7] Foct and Akdut^[6] investigated the microhardness of ferrite and austenite in DSS containing different nitrogen (N) contents and found that ferrite is harder than austenite if the nominal N content is less than 0.12 wt pct, whereas austenite is harder than ferrite if the nominal N content is higher than 0.12 wt pct, as the N content partitioned into austenite increased with an increase in the nominal N content, which promotes the solid-solution hardening of the austenite.

Meanwhile, the effect of N partitioning on the mechanical properties with an increase in the annealing temperature in DSS with the same nominal composition has not been reported despite the fact that it is conceivable that noticeable N partitioning can occur due to the change of the phase fraction with an increase in the annealing temperature. In addition, it is somewhat surprising that the effect of the grain growth during annealing on the mechanical properties has not been discussed or was overlooked in many previous works.^[1,4,5] The grain size of DSS increases with an increase in the annealing temperature. Therefore, the softening by grain growth should also be considered when evaluating the mechanical properties of annealed DSS.

Taking all these factors into account, here, we investigate the change in the yield strength of DSS with an increase in the annealing temperature in terms of the effect of N partitioning into austenite, the change of the phase fraction and the grain growth. The tensile properties and microstructure were evaluated using tensile tests, a scanning electron microscope (SEM) equipped with an electron backscatter diffraction (EBSD) attachment, and an electron probe micro analysis (EPMA). In addition, for a better understanding of the change of the hardness of the individual phases upon annealing, nanoindentation experiments were carried out.

The tensile properties of commercial DSS of SAF2205 and SAF2507, whose chemical compositions are given in Table I, were investigated. The SAF2507 alloy as a super DSS contains higher Cr, Ni, Mo, and N contents than SAF2205, resulting in higher pitting corrosion resistance which is expressed by the pitting resistance

MIN-HO JANG, Ph.D. Student, is with the Division of Materials Science and Engineering, Hanyang University, Seongdong-ku, Seoul 133-791, Republic of Korea, and also with the Ferrous Alloy Department, Advanced Metallic Materials Division, Korea Institute of Materials Science, 797 Changwondaero, Seongsangu, Changwon, Gyeongnam 642-831, Republic of Korea. JOONOH MOON, Senior Researcher, and TAE-HO LEE and SEONG-JUN PARK, Principal Researchers, are with the Ferrous Alloy Department, Advanced Metallic Materials Division, Korea Institute of Materials Science. Contact e-mail: mjo99@kims.re.kr HEUNG NAM HAN, Professor, is with the Department of Materials Science and Engineering, Seoul National University, Seoul 151-742, Republic of Korea.

Manuscript submitted August 5, 2013.

Article published online February 19, 2014

equivalent number (PREN, PREN = pct Cr + 3.3 pct Mo + 16 pct N). To achieve samples having different ratios of ferrite and austenite, SAF2205 and SAF2507 were annealed at various temperatures [SAF2205: 1271 K, 1403 K, and 1533 K (998 °C, 1130 °C, and 1260 °C), SAF2507: 1323 K, 1423 K, and 1533 K (1050 °C, 1150 °C, and 1260 °C)] for 1 hour and were subsequently quenched. The annealing temperatures to control the ratio of ferrite to austenite were selected based on the thermodynamic calculation using Thermo-Calc. (Version S, TCFE 6 database) as shown in Figure 1. The expected ratios of ferrite and austenite at the desired annealing temperature were approximately 4:6, 5:5, and 6:4, as shown in Table II. The tensile properties were assessed using a tensile test machine (INSTRON 5882, Canton, MA) at an ambient temperature at a nominal strain rate of $1.33 \times 10^{-3} \text{ s}^{-1}$, after which the yield strength was determined by the 0.2 pct

offset method. The microstructures of the annealed samples were observed using SEM (JSM-7001F) equipped with an EBSD (HKL Nordlys Channel 5). The average grain size and phase fraction were measured from the EBSD analysis. In this case, the average grain size was identified with a critical misorientation angle of 5 deg. For the EBSD analysis, the samples were electropolished (Struers Lectropol-5; Struers A/S, Ballerup) for 20 s in a mixed solution of 10 pct perchloric acid and 90 pct Methanol at -20 K (-20 °C) with an applied potential of 25 V. EPMA (JXA-8500F, JEOL) was carried out to examine the partitioning of the alloying elements as a function of the annealing temperature. To assess the change in the mechanical properties of the individual phase according to the annealing, nanoindentation experiments were performed at a peak load of 5 mN using a Hysitron Tribolab nanoindenter equipped with a Berkovich indenter.

Electron backscatter diffraction phase maps of SAF2205 and SAF2507 after annealing are shown in Figure 2. With an increase in the annealing temperature, the average grain size and ferrite fraction increased. Table II summarizes the measured results. The true stress–strain curves of the annealed samples are shown in Figure 3. The tensile properties of SAF2205 and SAF2507 exhibit different aspects with an increase in the annealing temperature; *i.e.*, the yield strength of SAF2205 decreased as the annealing temperature increases, while the reverse was true for SAF2507.

First, the decrease in the yield strength in SAF2205 may be due to softening caused by the grain growth despite the increase in the ferrite fraction, as shown in Table II. In the literature,^[3] the parameters of the Hall–Petch relationship to predict the yield strength of ferrite and austenite in DSS are presented as

$$\sigma = \sigma_0 + k \cdot d^{-1/2}, \quad [1]$$

where σ is the yield strength, d is the grain size, and σ_0 (60.5 ksi for ferrite and 19.5 ksi for austenite) and k (0.95 for ferrite and 1.45 for austenite) are constants. Assuming that the grain size is very large, like a single crystal, σ equals σ_0 in Eq. [1], indicating that σ_0 implies the intrinsic yield strength regardless of the grain boundary strengthening. Therefore, the higher σ_0 value in ferrite than austenite means that the yield strength of ferrite is higher than that of austenite, and it is expected that the yield strength of DSS can increase as the ferrite fraction increases if the grain size

Table I. Chemical Compositions of the SAF2205 and SAF2507 Alloys Examined in this Study, in Weight Percent

	C	Si	Mn	P	S	Cr	Ni	Mo	N
SAF 2205	0.016	0.39	1.38	0.024	0.001	22.44	5.73	3.24	0.186
SAF 2507	0.024	0.33	0.50	0.025	0.0004	25.58	7.19	3.76	0.272

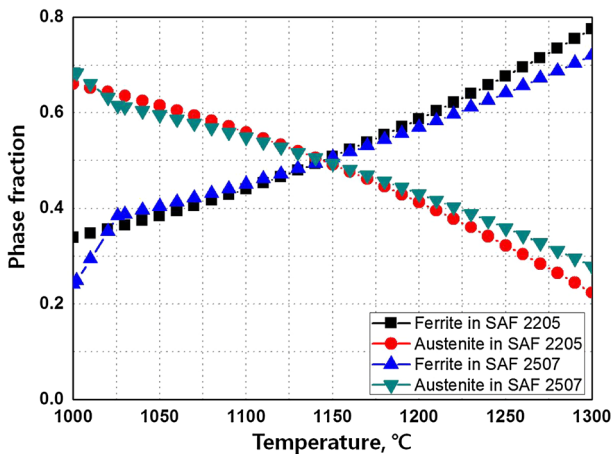


Fig. 1—Equilibrium phase fraction of austenite and ferrite with an increase in the temperature as calculated by Thermo-Calc.

Table II. Phase Fractions and Mean Grain Sizes of the Annealed Samples

Alloy	Annealing Temp. [K (°C)]	Phase Fraction				Measured Mean Grain Size (μm)	
		Calculated		Measured		α	γ
		α	γ	α	γ		
SAF 2205	1271 (998)	33.9	66.1	40.8	59.2	2.3	1.9
	1403 (1130)	48.0	52.0	47.4	52.6	8.5	2.2
	1533 (1260)	69.6	30.4	65.2	34.8	15.8	11.6
SAF 2507	1323 (1050)	40.4	59.6	42.7	57.3	2.7	2.4
	1423 (1150)	50.5	49.5	48.1	51.9	11.2	2.9
	1533 (1260)	65.6	34.4	55.9	44.1	14.1	9.7

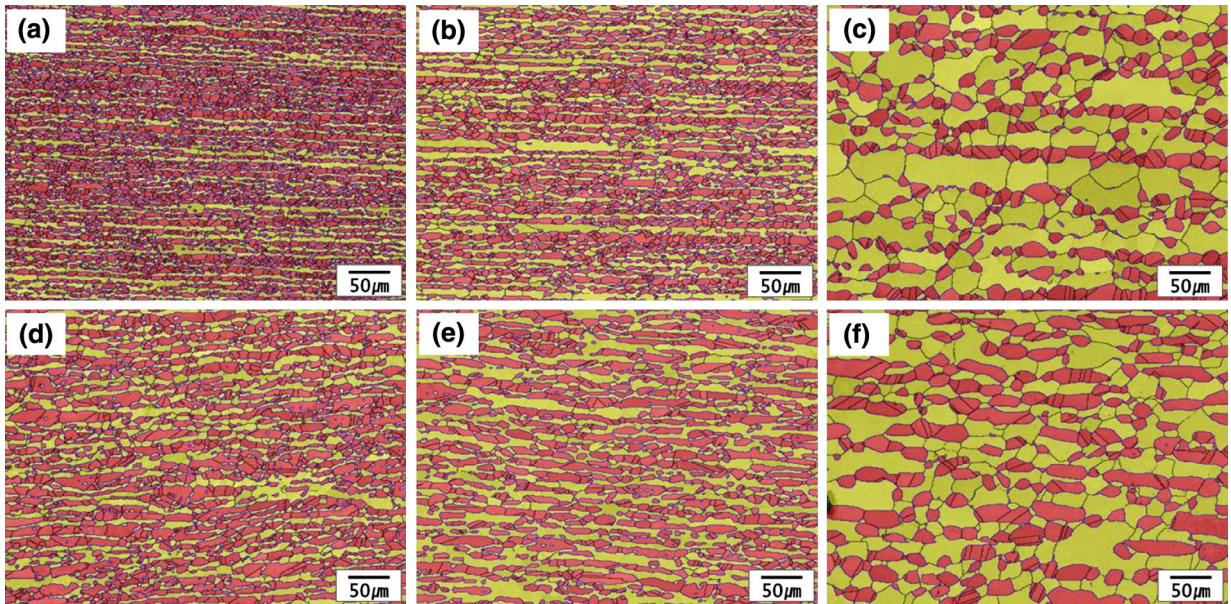


Fig. 2—EBSD phase map of the samples after annealing: (a) through (c) SAF 2205 annealed at 1271 K, 1403 K, and 1533 K (998 °C, 1130 °C, and 1260 °C), and (d) through (f) SAF2507 annealed at 1323 K, 1423 K, and 1533 K (1050 °C, 1150 °C, and 1260 °C). Body-centered cubic (■ BCC, ferrite); face-centered cubic (■ FCC, austenite); — misorientation angle >5 deg.

remains the same, as reported in the literature.^[1,3,5] However, the yield strength of SAF2205 decreased with an increase in the annealing temperature despite the increase of the ferrite fraction, as shown in Figure 3(a). This may be due to the softening effect by the grain growth. To confirm the effect of the phase fraction and the grain growth quantitatively, we calculate the yield strength of the single phases (ferrite and austenite) of SAF2205 as the annealing temperature increase using Eq. [1], and we measured the grain size, as shown in Table II. The yield strength of the mixed phases of SAF2205 was predicted by a simple rule of mixture^[8]; *i.e.*,

$$\sigma^d = f_\alpha \cdot \sigma_\alpha + f_\gamma \cdot \sigma_\gamma, \quad [2]$$

where σ^d is the yield strength of DSS, σ_α and σ_γ are, respectively, the yield strength of ferrite and austenite, f_α and f_γ are correspondingly the phase fraction of ferrite and austenite. Figure 4 shows the increment of the yield strength with an increase in the annealing temperature as compared to the yield strength of the samples annealed at 1271 K (998 °C) for SAF2205 and 1323 K (1050 °C) for SAF2507. The yield strength of SAF2205 decreased with an increase in the annealing temperature, showing good agreement with the results predicted by Eqs. [1] and [2]. The decrease of the yield strength of SAF2205 with an increase in the annealing temperature arose, because the softening effect by grain growth played a larger role than the hardening effect by the increasing ferrite fraction.

Next, we calculated the yield strength of SAF2507 using Eqs. [1] and [2] and compared the result with the measured data, as shown in Figure 4. In the case of SAF2507, the calculated yield strength decreases with an increase in the annealing temperature, like SAF2205, while the measured yield strength increased with an increase in the annealing temperature. As the annealing temperature increases, the changes of the values of the

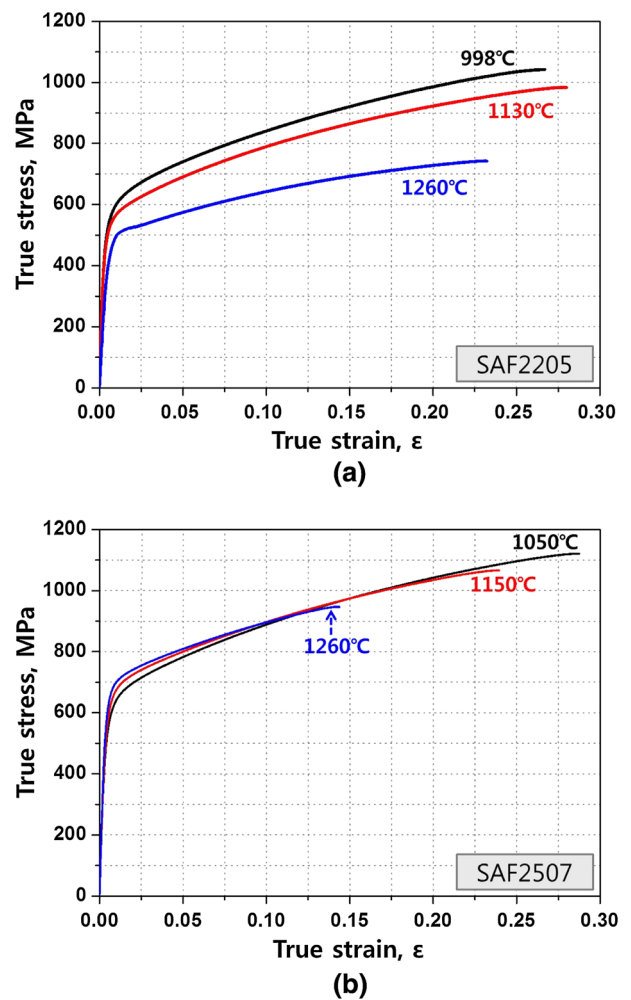


Fig. 3—True stress–strain response of the samples after annealing.

grain size and phase fraction of the SAF2507 samples are similar to those of the SAF2205 samples, as shown in Table II. Therefore, it is conceivable that the change of the yield strength due to the increase of the ferrite fraction and grain growth in SAF2507 is similar to this change of SAF2205. Nevertheless, the measured yield strength of SAF2507, unlike SAF2205, increased with an increase in the annealing temperature, implying that another factor besides the phase fraction and grain growth exists. Here, we are taking note of the partitioning of the alloying elements, especially N partitioning, according to the annealing treatment, as it can strongly affect the strength of ferrite and austenite.^[6,7,9,10] The partitioning of the alloying elements was analyzed using EPMA, as shown in Table III. Using the measured data of the phase fraction in Table II and the chemical composition in Table III, it is possible to calculate the total N contents by the simple equation

$$X^i = f_\alpha \cdot X_\alpha^i + f_\gamma \cdot X_\gamma^i, \quad [3]$$

where X^i , X_α^i , and X_γ^i are the total contents, the contents in ferrite and the contents in austenite of i

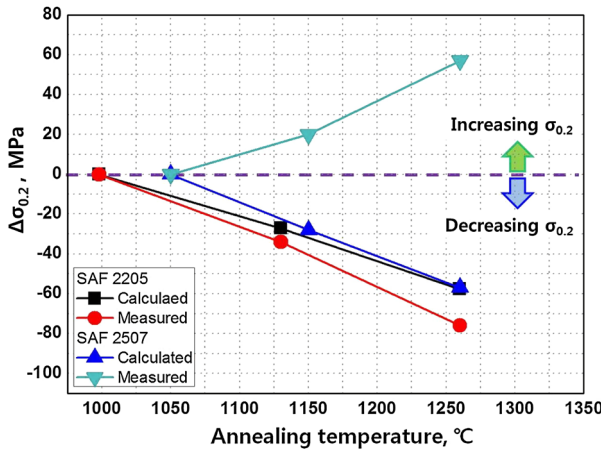


Fig. 4—Change in the 0.2 pct offset yield strength ($\sigma_{0.2}$) of the samples with an increase in the annealing temperature.

element, respectively. However, it is possible that the values calculated using Eq. [3] are slightly different, under 0.1 wt pct in the case of N, with the nominal composition shown in Table I. This difference can be understood as experimental error. A more important result in Table III is that the partitioning of N in SAF2507 was found to be noticeable, while the partitioning results of the other elements were insignificant. Figure 5 shows the measured N contents in the samples, indicating that N was gradually enriched into austenite with an increase in the annealing temperature. Meanwhile, the N partition in SAF2205 is much smaller than that of SAF2507; this is related to the smaller nominal N contents in the matrix, as shown in Table I.

To confirm the effect of the N partition on the strength of ferrite and austenite, the nanohardnesses of the ferrite and austenite in each sample were measured. Figure 6 shows representative nanoindentation load (P)–displacement (h) curves. The selection of the curves for the ferrite and austenite phase was made through observation of the EBSD phase maps of the hardness impressions and microstructures. In the case of SAF2205, the ferrite shows lower displacement than the austenite at the peak

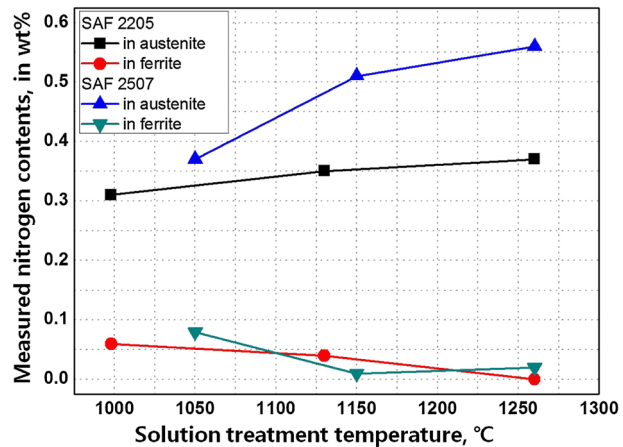


Fig. 5—EPMA analysis showing nitrogen partitioning in the samples after annealing.

Table III. Chemical Composition in Each Phase of the Annealed Samples as Measured by EPMA (Weight Percent)

Alloy	Annealing Temp. [K (°C)]	Phase	Chemical Composition Measured by EPMA (Wt Pct)					
			Mn	Cr	Ni	Mo	N	Fe
SAF 2205	1271 (998)	α	1.55	21.59	6.62	3.37	0.06	66.83
		γ	1.49	21.69	6.25	3.64	0.31	66.62
	1403 (1130)	α	1.44	22.44	5.12	4.01	0.03	66.98
		γ	1.55	19.92	7.40	2.67	0.30	68.16
SAF 2507	1533 (1260)	α	1.31	22.42	5.14	3.46	0.01	66.93
		γ	1.43	21.90	7.13	2.35	0.37	70.30
	1323 (1050)	α	0.40	26.16	6.41	4.99	0.08	61.98
		γ	0.48	25.61	7.10	4.07	0.37	62.38
SAF 2507	1423 (1150)	α	0.42	26.63	5.71	4.40	0.03	62.71
		γ	0.51	24.43	8.73	3.06	0.51	62.69
	1533 (1260)	α	0.44	24.94	6.43	4.05	0.02	64.21
		γ	0.47	24.36	8.37	2.95	0.56	63.29

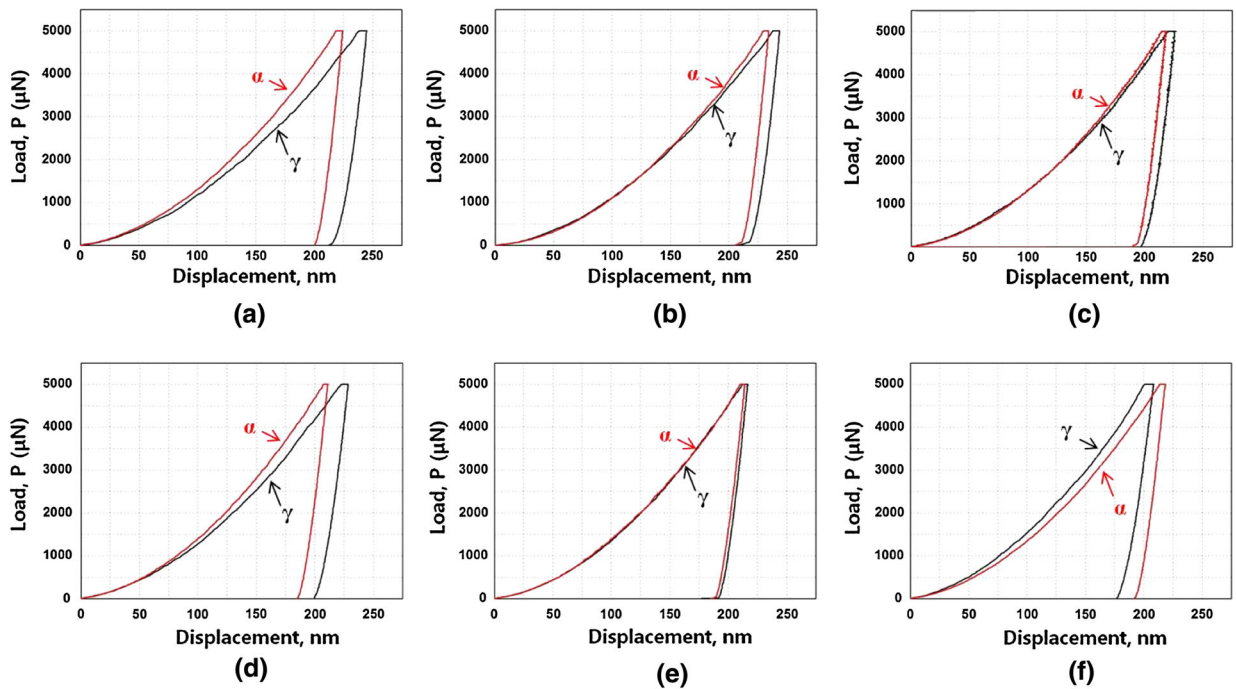


Fig. 6—Representative P - h curves of ferrite and austenite obtained by the nanoindentation test: (a) through (c) SAF2205 annealed at 1271 K, 1403 K, and 1533 K (998 °C, 1130 °C, and 1260 °C), and (d) through (f) SAF2507 annealed at 1323 K, 1423 K, and 1533 K (1050 °C, 1150 °C, and 1260 °C).

load regardless of the annealing temperature, implying that ferrite has higher hardness than austenite and that there is no considerable change of austenite hardness as the annealing temperature increases. On the other hand, the austenite of SAF2507 becomes stronger than ferrite with an increase in the annealing temperature. This hardening of austenite may be closely related to the N partitioning into austenite, as shown in Figure 5. In the References 11 through 13, it has been revealed that the nanoindentation hardness exhibited a linear relationship with the Vickers hardness and the intrinsic yield strength in Eq. [1]. Therefore, it is conceivable that the hardening of austenite with an increase in the annealing temperature shown in Figure 6 can clearly affect the enhancement of the yield strength of SAF2507.

Previous research^[14] reported that an increase of 0.2 wt pct N in DSS contributes to an increase of the yield strength above 100 MPa; this level well corresponds to the difference between the measured and calculated values of the yield strength observed in SAF2507 shown in Figure 5. On the other hand, in the case of SAF2205, a small increase of N (≈ 0.06 wt pct) in austenite occurred; thus, remarkable hardening by N partitioning did not take place as shown in Figures 3 and 4.

The change of the yield strength of DSS at different annealing temperatures was evaluated, and the following conclusions were drawn.

(1) The phase fraction and the mean grain size were measured by EBSD analysis, showing that the austenite fraction decreased and the mean grain size of both the austenite and ferrite increased with an increase in the annealing temperature.

(2) An EPMA analysis showed that N was partitioned into austenite with a decrease in the austenite fraction. In addition, remarkable N partitioning was observed in SAF2507, which contained a higher nominal N content as compared with SAF2205.

(3) The microhardness of both ferrite and austenite was measured through a nanoindentation test. The microhardness of austenite increased due to N partitioning with an increase in the annealing temperature, and the austenite became stronger than the ferrite when the N content partitioned into austenite was higher than 0.5 wt pct. Therefore, when the yield strength of the austenite is low, the yield strength decreased with an increase in the annealing temperature due to softening caused by the grain growth. However, when the N enrichment of the austenite is high (>0.5 pct in this study), the yield strength increased due to the noticeable hardening of austenite with an increase in the annealing temperature despite the grain growth.

This research was supported by a grant from the Fundamental R&D Program for Core Technology of Materials funded by the Ministry of Knowledge Economy, Republic of Korea. The work of one author (H.N.H.) was supported by Basic Science Research Program through the National Research Foundation

of Korea (NRF) funded by the Ministry of Science, ICT and Future Planning (2013008806). The authors wish to thank Yong-Min Kim for his valuable support for the nanoindentation test.

REFERENCES

1. Y.-H. Park and Z.-H. Lee: *Mater. Sci. Eng. A*, 2001, vol. 297, pp. 78–84.
2. J.O. Nilsson: *Mater. Sci. Technol.*, 1992, vol. 8, pp. 685–700.
3. S. Floreen and H.W. Hyden: *Trans. ASM*, 1968, vol. 61, pp. 489–99.
4. R. Badji, M. Bouabdallah, B. Bacroix, C. Kahloun, B. Belkessa, and H. Maza: *Mater. Charact.*, 2008, vol. 59, pp. 447–53.
5. K. Unnikrishnan and A.K. Mallik: *Mater. Sci. Eng.*, 1987, vol. 94, pp. 175–81.
6. J. Foct and N. Akdut: *Scripta Metall.*, 1993, vol. 29, pp. 153–58.
7. J.J. Moverare and M. Odén: *Metall. Mater. Trans. A*, 2002, vol. 33A, pp. 57–71.
8. W. Horvath, B. Tabernig, E. Werner, and P. Uggowitzer: *Acta Mater.*, 1997, vol. 45, pp. 1645–54.
9. J.W. Simons: *Acta Mater.*, 1997, vol. 45, pp. 2467–75.
10. K. Orita, Y. Ikeda, T. Iwadate, and J. Ishizaka: *ISIJ Int.*, 1990, vol. 30, pp. 587–93.
11. J.-H. Kim, T. Tabaru, and H. Hirai: *Mater. Trans. JIM*, 2003, vol. 44, pp. 673–76.
12. T. Ohmura, K. Tsuzaki, and S. Matsuoka: *Scripta Mater.*, 2001, vol. 45, pp. 889–94.
13. M. Gaško and G. Rosenberg: *Mater. Eng./Mater. Inž.*, 2011, vol. 18, pp. 155–59.
14. R.A. Varin and K.J. Kurzydowski: *Mater. Sci. Eng.*, 1998, vol. 101, pp. 221–26.